University of Wisconsin Milwaukee
UWM Digital Commons

Theses and Dissertations

August 2017

The Potential Role of AIRAP/AIRAPL in Ameliorating the Toxicity Related to Amyloid-beta (aβ) in Mammalian Neuronal Cells

Advaita Chakraborty
University of Wisconsin-Milwaukee

Follow this and additional works at: https://dc.uwm.edu/etd

Part of the Medicine and Health Sciences Commons

THE POTENTIAL ROLE OF AIRAP/AIRAPL IN AMELIORATING THE TOXICITY

RELATED TO AMYLOID-BETA (Aβ) IN MAMMALIAN NEURONAL CELLS

by

Advaita Chakraborty

A Thesis Submitted in

Partial Fulfillment of the

Requirements for the Degree of

Master of Science

in Biomedical Sciences

at

The University of Wisconsin-Milwaukee

August 2017

ABSTRACT

THE POTENTIAL ROLE OF AIRAP/AIRAPL IN AMELIORATING THE TOXICITY
RELATED TO AMYLOID-BETA (Aβ) IN MAMMALIAN NEURONAL CELLS

by

Advaita Chakraborty

The University of Wisconsin-Milwaukee, 2017
Under the Supervision of Professor Wail Hassan

Alzheimer's disease is an irreversible and progressive brain disorder that affects memory and

thinking skills. It is considered to be one of the most important causes of dementia in older

adults. The disease is accompanied by accumulation of amyloid beta (Aβ) plaques in the brains

of patients and presence of neurofibrillary tangles (NFTs) in the nerve tissue. The tangles are

formed by a protein known as protein-tau (p-tau). Aβ plaques are responsible for

neurodegeneration, cognitive decline, and loss of memory in patients affected with Alzheimer's

disease. It is estimated that Alzheimer's disease ranks third, just behind heart disease and cancer,

as a cause of death for the elderly in the United States. AIRAP and AIRAPL are ubiquitin-

binding proteins that are thought to enhance the function of the proteasome by clearing out the

misfolded proteins from the brain. Previous studies have shown that AIP-1 (a homologue of

AIRAP and AIRAPL) was overexpressed in a *Caenorhabditis elegans* disease model which in

turn helped to reduce the accumulation of Aβ and thus had a protective effect against Aβ

toxicity. The purpose of our study is to test whether AIRAP and AIRAPL are protective against

the toxicity associated with Aβ in mammalian neuronal cells. We are hypothesizing that AIRAP

and AIRAPL are protective against Aβ toxicity in HT22 hippocampal cells, which would significantly decelerate the progression of Alzheimer's disease. We have manipulated the expression of AIRAP and AIRAPL and studied the effect of overexpression and knockdown on Aβ toxicity. Overexpression was achieved by establishing transfected cell lines overexpressing AIRAP and AIRAPL with help of a CMV constitutive promoter. On the other hand, knockdown of genes was attained using specific DsiRNA. Using Trypan Blue staining, we found that cell lines overexpressing AIRAP/AIRAPL could lower Aβ toxicity, thus increasing the number of viable cells. Additionally, knocking down AIRAP/AIRAPL expression appeared to worsen the condition of cells, as the number of dead cells increased, in response to Aβ treatment. With help of real-time PCR, mRNA levels of AIRAP and AIRAPL was measured. It was shown that expression of both AIRAP and AIRAPL was enhanced during the initial stages of induction in cell line having induced Aβ. However, as the induction time increased, the expression levels started to fall off. Further studies are essential to know the exact mechanism behind AIRAP/AIRAPL protection against Aβ toxicity.

iv

TABLE OF CONTENTS

LIST OF TABLES

LIST OF ABBREVIATIONS

AD   Alzheimer's disease

MCI   Mild cognitive impairment

NFTs   Neurofibrillary tangles

Aβ   Beta-amyloid protein

p-tau   Protein tau

AβPP   Beta-amyloid precursor protein

CSF   Cerebrospinal fluid

BBB   Blood brain barrier

PQC   Protein quality control system

HSPs   Heat shock proteins

AIRAP   Arsenite-inducible RNA-associated protein

AIRAPL   AIRAP-like protein

CMV   Cytomegalovirus

DsiRNA   Dicer-substrate interfering RNA

ROS   Reactive oxygen species

DMEM   Dulbecco's modified eagle's medium

FBS   Fetal bovine serum

GFP	Green fluorescent protein
PBS	Phosphate buffer saline
cDNA	Complementary DNA
NC	Negative control

ACKNOWLEDGEMENTS

INTRODUCTION

Alzheimer's Disease: Global impact, symptoms, and causes

Alzheimer's disease (AD) is the most common cause of dementia in the elderly (1). The disease affects around 75% of the 35 million people suffering from dementia worldwide. It is estimated that by the year 2050, around 115 million people will be affected by AD, since the number is increasing at a fast pace every year (2). In developing Countries, it has been reported that 1 out of each 10 individuals who are 65 years of age or older and one-third of those who are over 85 years old, suffer from some form of dementia (2). Mild cognitive impairment (MCI) is a term that includes a broad spectrum of cognitive impairment syndromes that precedes AD and dementia (3). It often depicts a transitional phase between normal aging and dementia (4). The disease leads to cognitive defects that affects memory, judgment, insight, and language functions (5). In aging, cognitive decline is a common feature and it is observed that changes in cognition represents early signs of neurodegenerative disease, ultimately leading to dementia (4). Furthermore, weight loss is common in Alzheimer's patients and this could be a marker of approaching AD in people with MCI (3). A clinical and community-based study showed that around 40% patients with AD have sleep disturbances (6).

AD, similar to all kinds of dementia, is caused by death of brain cells. With time, the total brain size shrinks since the tissue has fewer nerve cells and connections (7). Postmortem/autopsy reports showed that tiny inclusions known as plaques and neurofibrillary tangles (NFTs) are present in the nerve tissue. Plaques are found between the dying cells in the brain. These plaques are formed from a protein called beta-amyloid (Aβ) (7). The tangles are found intracellularly in the brain neurons either from hyperphosphorylation of protein tau (p-tau) or disintegration of p-tau, which is a tubulin-associated protein (7). The deposition of Aβ leads to the initial

1

neurodegenerative and neurotoxic cascade and relates strongly with decreased cognitive performance in an individual (1). The main underlying causes of neurodegeneration, cognitive decline, and memory loss are the presence of Aβ and tau-related neuropathies in the brains of patients. Aβ peptides are 39-43 amino acid peptides that are derived from the proteolytic hydrolysis of amyloid-β precursor protein (AβPP) in neurons and other cell types. (8). The presence of NFTs is accompanied by gliosis, loss of neurons and synapses (9). Aβ and p-tau lead to chronic inflammatory response and oxidative damage, resulting in progressive neuronal degeneration (10). It has been shown that there is a decrease in $A\beta_{42}$ levels in the cerebrospinal fluid (CSF) and an increase in CSF p-tau levels that can be a biomarker of pathologic changes in the brain that ultimately lead to AD or increases the risk of developing the disease. These changes have been associated in patients with MCI who eventually will develop AD later in life (11).

Clearance of Aβ and importance of Proteasome

There are three pathways that help to clear Aβ from the brain. They are: transport across blood-brain barrier (BBB), degradation in the brain tissue, and bulk flow of cerebrospinal fluid (CSF). However, clearance across BBB is considered to be the most efficient for removing Aβ (8). It is believed that accumulation of Aβ in AD patients is due to inadequate Aβ elimination, with patients showing less than 30% clearance of Aβ from the brain (1). The level of Aβ in the brain is determined by its production and clearance. The imbalance occurs between the two processes that leads to accumulation of Aβ in the brain (8). It is believed that age-related accumulation of damaged proteins result both from increased damage and lower efficiency of degradative systems. The proteasome system most often helps in clearing the oxidatively modified proteins

and it is the main pathway that removes damaged proteins and it is responsible for maintaining the proteostasis especially during stress conditions (12).

However, proteasome function declines with age in various cell types and organs, and this has been shown in various studies. As a result, decline in the activity of proteasome results in accumulation of oxidized proteins (12). There are significant implications on various neurodegenerative diseases due to the reduction in the activity of proteasome and other intracellular proteolytic machineries (12). Ubiquitin-proteasome system, a part of the protein quality control system (PQC), helps to degrade misfolded or damaged proteins and removes proteins involved in various cellular processes, such as, signal transduction, regulation of cell cycle, cell death, and finally regulates gene transcription. This system uses two strategies in order to maintain protein homeostasis during protein misfolding (12). Misfolded proteins can be refolded back in order to recover the normal conformation. Molecular chaperons, such as heat shock proteins (HSPs), play a vital role in protein refolding (12). In other cases, the proteins are directed towards the ubiquitin-proteasome system for degradation (12).

Structurally, the 26S proteasome holocomplex consists of a 20S catalytic core and a 19S regulatory cap on either end. The 20S subunit has four stacked rings that form a barrel-shaped molecule with a central cavity (13). The α-rings are the outer two non-catalytic rings and the two catalytic inner rings are known as β-rings. There are three proteolytic activities that are confined to the β-rings, chymotrypsin-like, caspase-like, and trypsin-like. (13).

Figure 1: 26S proteasome holocomplex

Growing evidences support that impaired proteostasis result in the increase of unfolded/misfolded proteins and formation of protein aggregates, which plays a vital role in the pathology of AD (14). In addition, a study demonstrated that Aβ oligomers, but not monomers, inhibited the activity of the proteasome in 3xTg-AD mice (pathology of AD is studied in this type of mice) when there are high levels of the oligomers present. Also, it was shown that there was accumulation of both Aβ and tau proteins when the activity of proteasome was inhibited (15). As a result, the proteasome is a vital pathway that links Aβ and tau pathology. Hence, it has been postulated that the function of the proteasome needs to be enhanced, so that the Aβ could be effectively cleared from the brain (15).

Function of AIRAP/AIRAPL including earlier studies

Arsenite-inducible RNA-associated protein (AIRAP) and AIRAP-like protein (AIRAPL) are ubiquitin-binding proteins that help to enhance the activity of proteasome in response to stress (16). It is demonstrated that functional impairment of AIP-1, a homologue of AIRAP and AIRAPL leads to acceleration in aging and protein aggregation in *Caenorhabditis elegans* disease model (16). In another study, AIP-1 was shown to be overexpressed in *C. elegans* in

4

what appeared to be a protective response against Aβ toxicity that led to reducing the accumulation of Aβ. Moreover, it was noted that transgenic expression of AIRAPL, but not AIRAP expression inhibited the toxicity related to Aβ in the worm model (17). It is evident from this study that AIRAP did not have a protective effect against Aβ toxicity in the worm model. But, it is not necessary that it won't be having any neuroprotective effect in mammals. Hence, we want to use both AIRAP and AIRAPL and study the effects they have related to Aβ toxicity in the cells.

OVERALL GOAL

The goal of this study is to test whether AIRAP and AIRAPL are protective against Aβ toxicity in mammalian neuronal cells. In order to test whether AIRAP and AIRAPL are protective, we will manipulate the expression of the two genes to test the effect of overexpression and knockdown on Aβ toxicity.

INNOVATION/ IMPACT

Drug targets that enhance the expression of AIRAP/AIRAPL that in turn reduce the toxicity related to Aβ could be a potential therapeutic drug target used in case of Alzheimer's patients. Hence, if AIRAP/AIRAPL offer protection against Aβ toxicity via enhanced proteasomal function in mammalian system, it would be useful in decelerating the progression of AD.

HYPOTHESIS AND SPECIFIC AIMS

The central hypothesis of this study was that **AIRAP and AIRAPL genes are protective against Aβ toxicity.** To examine this hypothesis, I proposed the following specific aims:

Specific Aim 1: To determine Aβ toxicity in mammalian neuronal cells. The working hypothesis of this aim: Aβ increases cell death and lowers the cell viability in the neuronal cells.

Specific Aim 2: To determine whether AIRAP/AIRAPL genes reduce cell death/ improve cell viability. The working hypothesis of this aim: AIRAP/AIRAPL improve cell viability of neuronal cells.

Specific Aim 2.1: To investigate the effect of overexpression of AIRAP/AIRAPL on cell viability. The working hypothesis of this aim: Overexpression of AIRAP/AIRAPL reduces cell death and increases the viability of cells. Overexpression was achieved by establishing stably transfected cell lines overexpressing AIRAP or AIRAPL using a cytomegalovirus (CMV) constitutive promoter.

Specific Aim 2.2: To determine the effect of knock down of AIRAP/AIRAPL on the cell viability. The working hypothesis of this aim: Knocking down AIRAP/AIRAPL increases the cell death and there was lower number of viable cells present. Knock down was achieved using specific dicer-substrate interfering RNA (DsiRNA).

Specific Aim 3: To ascertain the over-expression of AIRAP/AIRAPL in presence of induced Aβ. The working hypothesis of this aim: AIRAP/AIRAPL were found to be overexpressed in presence of Aβ in mammalian neuronal cells.

MATERIALS AND METHODS

Construction of Plasmids

We have constructed various plasmids containing either AIRAP or AIRAPL gene. Plasmids pWH017, pWH018, and pWH019 possess different variants of the human Amyloid-β precursor protein (APP) gene. Next, we transfected the plasmids into the HT22 neuronal cells and studied the effects of the genes when overexpressed/ knocked out in presence of Aβ treatment. Moreover, we also designed plasmids without AIRAP and AIRAPL genes (pWH020 and pWH021 respectively) that served as controls. Detailed description of the plasmids is provided below.

- **pWH013 (9853 bp):** This was constructed using plasmid pWH002 (containing human CMV promoter and AIRAP gene) and cut with HindIII enzyme (New England Biolabs, Ipswich, MA, Cat. No. R3104S). The product of 6557 bp was ligated with the PCR products of AcGFP (template: pAcGFP1-Hyg-N1 and primers: CL-AcGFP1-F and CL-AcGFP1-R) of 1625 bp and Hygromycin (template: pAcGFP1-Hyg-N1 and primers: CL-Hygromycin-F and CL-Hygromycin-R) of 1725 bp. Cloning was performed using NEBuilder Assembly (HiFi DNA Master Mix: New England Biolabs, Ipswich, MA, Cat. No. M5520S; NEBuilder Positive Control: New England Biolabs, Ipswich, MA, Cat. No. N2611A). Transformation was done using high efficiency competent 5α *E. coli* cells (New England Biolabs, Ipswich, MA, Cat. No. C2987H; SOC Medium: New England Biolabs, Ipswich, MA, Cat. No. B9020S; pUC 19 Control DNA: New England Biolabs, Ipswich, MA, N3041A).

Figure 2. Plasmid pWH013

▪ **pWH014 (10189 bp):** Plasmid pWH001 (presence of human CMV promoter and AIRAPL gene) was cut with HindIII enzyme (New England Biolabs, Ipswich, MA, Cat. No. R3104S) and the product of 6557 bp was ligated with the PCR products of AcGFP (1625 bp) and Hygromycin (1725 bp). This was done with help of NEBuilder Assembly (HiFi DNA Master Mix: New England Biolabs, Ipswich, MA, Cat. No. M5520S; NEBuilder Positive Control: New England Biolabs, Ipswich, MA, Cat. No. N2611A). Transformation was carried out using high efficiency competent 5α *E. coli* cells (New England Biolabs, Ipswich, MA, Cat. No. C2987H; SOC Medium: New England Biolabs, Ipswich, MA, Cat. No. B9020S; pUC 19 Control DNA: New England Biolabs, Ipswich, MA, N3041A).

8

Figure 3. Plasmid pWH014

- **pWH015 (9782 bp):** This was prepared by cutting pWH013 with NotI enzyme (New England Biolabs, Ipswich, MA, Cat. No. R3189S). The product of 7931 bp was ligated with the PCR products of DsRed (template: pCL148 and primers: CL-DsRed-F and CL-DsRed-R) of 703 bp and AIRAP (template: AIRAP. PolyA + CMV promoter and primers: CL-NotI-PolyA+CMV-KpnI-F and CL-NotI-PolyA+CMV-KpnI-R) of 1201 bp using NEBuilder Assembly (HiFi DNA Master Mix: New England Biolabs, Ipswich, MA, Cat. No. M5520S; NEBuilder Positive Control: New England Biolabs, Ipswich, MA, Cat. No. N2611A). Similarly, transformation was carried out using high efficiency competent 5α *E. coli* cells

(New England Biolabs, Ipswich, MA, Cat. No. C2987H; SOC Medium: New England Biolabs, Ipswich, MA, Cat. No. B9020S; pUC 19 Control DNA: New England Biolabs, Ipswich, MA, N3041A).
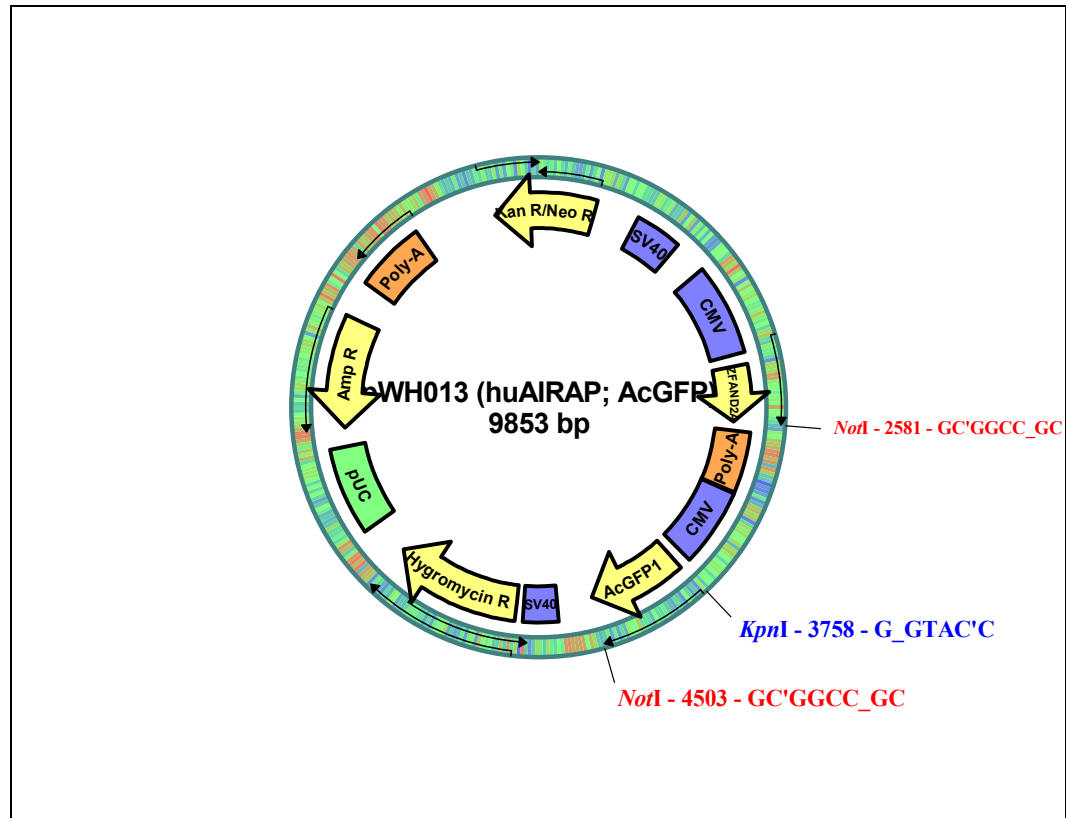

Figure 4. Plasmid pWH015

- **pWH016 (10118 bp):** The plasmid was constructed using pWH014 that was cut by SpeI enzyme (New England Biolabs, Ipswich, MA, Cat. No. R3133S) + HindIII enzyme (New England Biolabs, Ipswich, MA, Cat. No. R3104S) and pWH015 was cut with SpeI enzyme (New England Biolabs, Ipswich, MA, Cat. No. R3133S) + HindIII enzyme (New England Biolabs, Ipswich, MA, Cat. No. R3104S). The 2597 bp fragment containing the AIRAPL gene from pWH014 was ligated with the 7521 bp fragment of pWH015 that had DsRed in it. The ligation

was carried out using DNA Quick Ligase enzyme (New England Biolabs,

Ipswich, MA, Cat. No. M2200S). Furthermore, transformation was performed

using high efficiency competent 5α *E. coli* cells (New England Biolabs, Ipswich,

MA, Cat. No. C2987H; SOC Medium: New England Biolabs, Ipswich, MA, Cat.

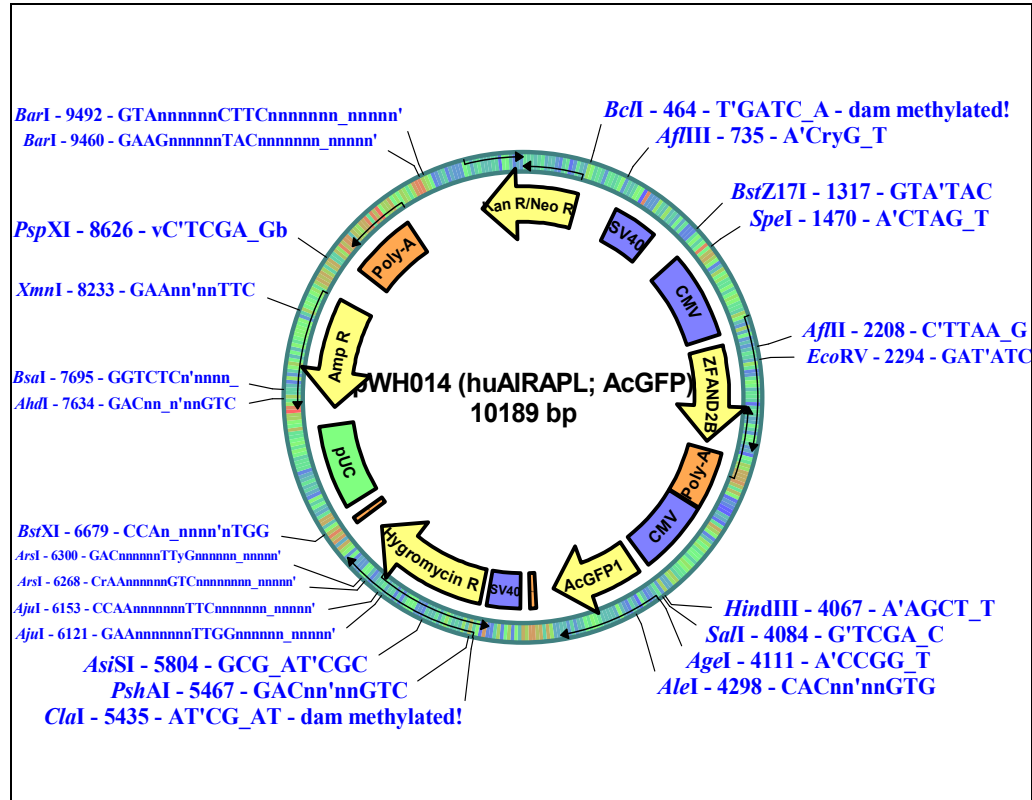No. B9020S; pUC 19 Control DNA: New England Biolabs, Ipswich, MA,

N3041A).

.**Figure 5. Plasmid pWH016**

▪ **pWH017** (**12272 bp**)**:** This was prepared by using pWH004-25 (containing

human Amyloid Precursor Protein wild-type variant 3) that was cut with SapI

enzyme (New England Biolabs, Ipswich, MA, Cat. No. R0569S). The product of

6773 bp was ligated with the PCR products of Tet3G (template: pCMV-tet3G and

primers: CL-TetOn3G-F and CL-TetOn3G-R) of 2118 bp and Puromycin

(template: pLVX-EF1a-IResPuro and primers: CL-Puromycin-F and CL-

Puromycin-R) of 3431 bp using NEBuilder Assembly (HiFi DNA Master Mix:

New England Biolabs, Ipswich, MA, Cat. No. M5520S; NEBuilder Positive

Control: New England Biolabs, Ipswich, MA, Cat. No. N2611A). Transformation

was performed by using high efficiency competent 5α *E. coli* cells (New England

Biolabs, Ipswich, MA, Cat. No. C2987H; SOC Medium: New England Biolabs,

Ipswich, MA, Cat. No. B9020S; pUC 19 Control DNA: New England Biolabs,
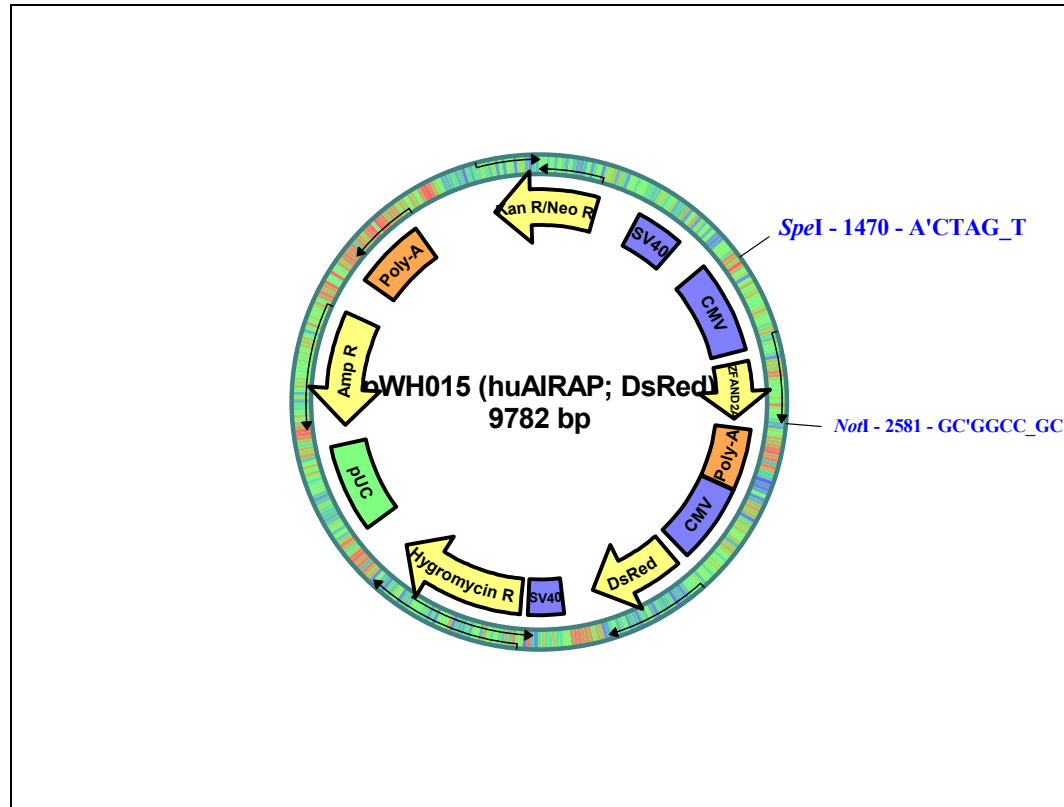
Ipswich, MA, N3041A).

Figure 6. Plasmid pWH017

- **pWH018:** The plasmid was prepared by cutting pWH004-M31 (presence of human Aβ G37L variant 3) with SapI enzyme (New England Biolabs, Ipswich, MA, Cat. No. R0569S). The product of 6773 bp was ligated with the PCR products of Tet3G (2118 bp) and Puromycin (3431 bp) with help of NEBuilder Assembly (HiFi DNA Master Mix: New England Biolabs, Ipswich, MA, Cat. No. M5520S; NEBuilder Positive Control: New England Biolabs, Ipswich, MA, Cat. No. N2611A). Transformation was carried out using high efficiency competent 5α *E. coli* cells (New England Biolabs, Ipswich, MA, Cat. No. C2987H; SOC Medium: New England Biolabs, Ipswich, MA, Cat. No. B9020S; pUC 19 Control DNA: New England Biolabs, Ipswich, MA, N3041A).
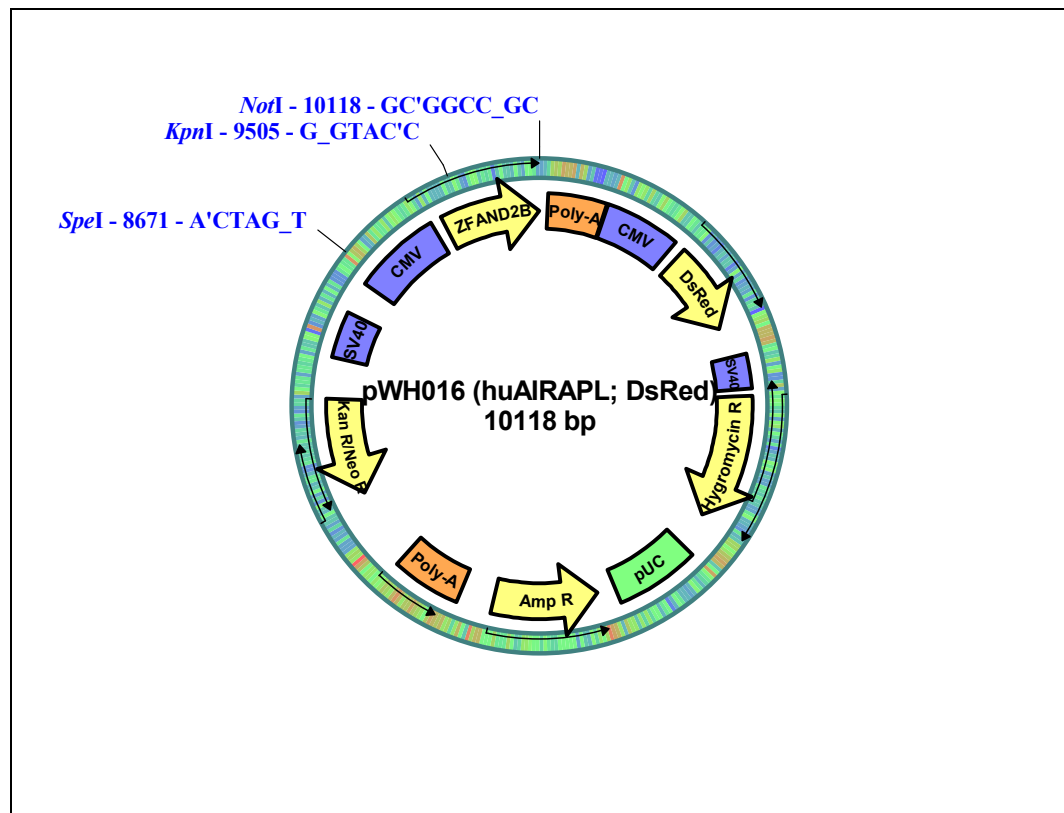
- .**pWH019:** This plasmid was constructed by cutting pWH004-32 (human Amyloid Precursor Protein Swedish variant 3) with SapI enzyme (New England Biolabs, Ipswich, MA, Cat. No. R0569S). Product of 6773 bp was ligated with the PCR products of Tet3G (2118 bp) and Puromycin (3431 bp) using NEBuilder Assembly (HiFi DNA Master Mix: New England Biolabs, Ipswich, MA, Cat. No. M5520S; NEBuilder Positive Control: New England Biolabs, Ipswich, MA, Cat. No. N2611A). For transformation, high efficiency competent 5α *E. coli* cells (New England Biolabs, Ipswich, MA, Cat. No. C2987H; SOC Medium: New England Biolabs, Ipswich, MA, Cat. No. B9020S; pUC 19 Control DNA: New England Biolabs, Ipswich, MA, N3041A) were used.

- **pWH020 (8163 bp):** This was prepared by using pWH013, cut with SacI enzyme (New England Biolabs, Ipswich, MA, Cat. No. R3156S) to remove the AIRAP gene. The larger fragment (containing AcGFP) was ligated using DNA Quick Ligase enzyme (New England Biolabs, Ipswich, MA, Cat. No. M2200S). The plasmid was used as a negative control. Consequently, transformation was carried out using high efficiency competent 5α *E. coli* cells (New England Biolabs, Ipswich, MA, Cat. No. C2987H; SOC Medium: New England Biolabs, Ipswich, MA, Cat. No. B9020S; pUC 19 Control DNA: New England Biolabs, Ipswich, MA, N3041A) were used.
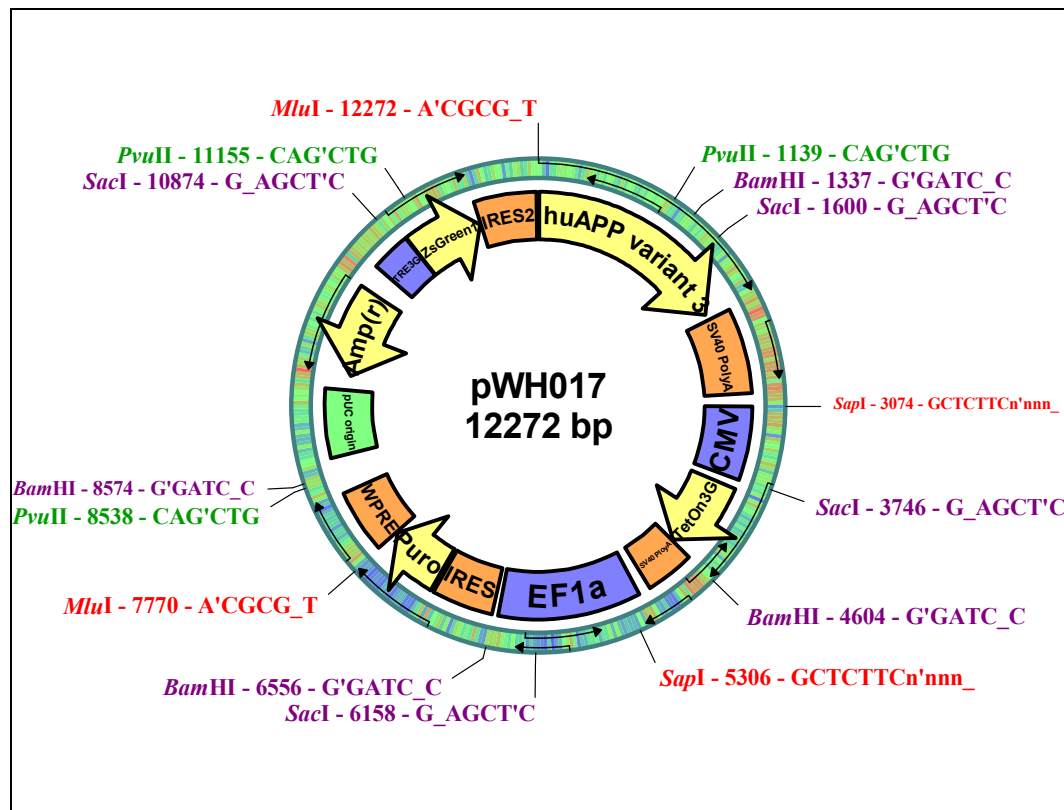

Figure 7. Plasmid pWH020

- **pWH021 (8092 bp):** Another negative control plasmid that was constructed by cutting pWH015 using SacI enzyme (New England Biolabs, Ipswich, MA, Cat. No. R3156S). DsRed gene was present in the larger fragment and the two ends were ligated using DNA Quick Ligase enzyme (New England Biolabs, Ipswich, MA, Cat. No. M2200S). Finally, transformation was performed using high efficiency competent 5α *E. coli* cells (New England Biolabs, Ipswich, MA, Cat. No. C2987H; SOC Medium: New England Biolabs, Ipswich, MA, Cat. No. B9020S; pUC 19 Control DNA: New England Biolabs, Ipswich, MA, N3041A).
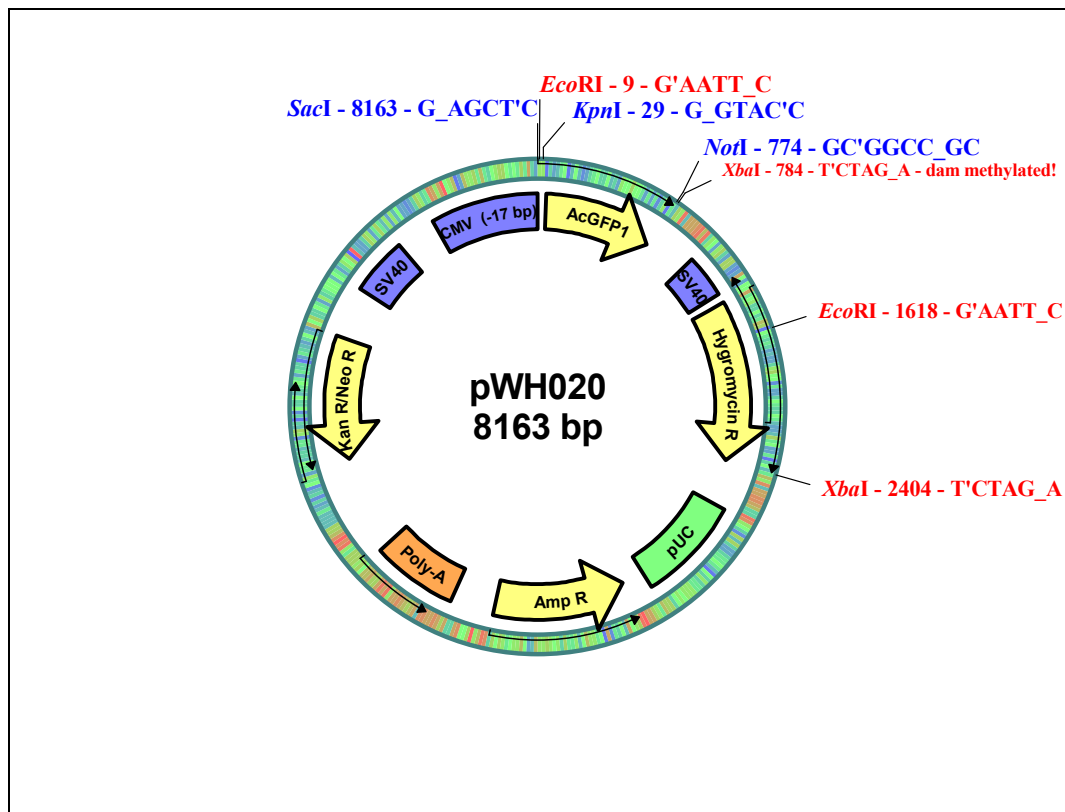

Figure 8. Plasmid pWH021

Plasmid DNA extraction

Transformation gave rise to bacterial colonies, those were picked and grown overnight in presence of LB media (Difco™ LB AGAR, MILLER, Becton Dickson and Company, Sparks, MD, Cat. No. 244520) containing Ampicillin (ThermoFisher Scientific, Waltham, MA, Cat. No. 11593027). 1 ml of 100 mg/ml Ampicillin was added to 1 L of LB media (40 g of LB AGAR powder was dissolved in Milli-Q water to make up the total volume up to 1 L). Finally, plasmid DNA was extracted using Monarch Plasmid Miniprep kit (New England Biolabs, Ipswich, MA, Cat. No. T1010S) following the manufacturer's instructions.

HT22 cells

The hippocampus is a vital component of the brains of humans and other mammals that plays essential roles in long-term memory and spatial navigation. The hippocampus is one of the first regions of the brain to get affected by AD, along with problems related to memory and disorientation (18). HT22 cells, an immortalized mouse hippocampal cell line, have been widely used as *in vitro* model for studying the mechanism of oxidative stress-induced neuronal cell death (19). Additionally, it is known that glutamate is the main endogenous excitatory neurotransmitter in the central nervous system. But, high concentrations of this neurotransmitter are associated with neurotoxicity and might be involved in various neurodegenerative disorders, such as Alzheimer's and Parkinson's disease (20). Mechanisms of glutamate toxicity involve enhanced production of reactive oxygen species (ROS). In HT22 cells, elevated ROS levels result in lipid peroxidation, protein oxidation, DNA damage, and ultimately cell death (20). Thus, HT22 cell line has been mainly used to study glutamate-induced nonreceptor-mediated neurotoxicity (20).

Transfection

HT22 mouse hippocampal cells were seeded 24 hours prior to transfection in a 48-well plate. Transfection was carried out the following day with help of chemical method. 1.5 µl of Lipofectamine™ 3000 reagent (INVITROGEN, Carlsbad, CA, Cat. No. L3000001) was diluted with 25 µl of OPTI-MEM™ medium (Gibco, Life Technologies, Gaithersburg, MD, Cat. No. 31985062) in one of the microcentrifuge tubes. 1 µg of plasmid DNA was diluted in 50 µl of OPTI-MEM™ medium, then 2 µl of P3000™ reagent (INVITROGEN, Carlsbad, CA, Cat. No. L3000001) was added and mixed thoroughly. This mixture was then added to the diluted Lipofectamine™ 3000 reagent after which it was incubated for 10-15 minutes. Finally, DNA-lipid complex was added to the neuronal cells. This was being performed by a lab mate. The transfected cells were analyzed after 48 hours.

Cell lines

We grew and maintained the following cell lines in order to test our overall goal.

- WH1: HT22; pTRE3G_ Zs Green + pCMV_ Tet3G (transactivator)
- WH2: HT22; pWH003 (pTRE3G_ Zs Green + Aβ) + pCMV_ Tet3G
- WH3: HT22; pWH017
- WH4: HT22; pWH018
- WH5: HT22; pWH019
- WH6: HT22; pWH013
- WH7: HT22; pWH014
- WH8: HT22; pWH015

- WH9: HT22; pWH016

- WH10: HT22; WH1 + pWH021

- WH11: HT22; WH1 + pWH015

- WH12: HT22; WH1 + pWH016

- WH13: HT22; WH2 + pWH021

- WH14: HT22; WH2 + pWH015

- WH15: HT22; WH2 + pWH016

- WH16: HT22; pWH020

- WH17: HT22; pWH021

- WH18: HT22; pWH020 + pWH021

Culture of cell lines

Cells were grown in Dulbecco's Modified Eagle's Medium (DMEM, CORNING, Corning, NY, Cat. No. 10-013-CV) with 10% fetal bovine serum (FBS, Sigma, St. Louis, MO, Cat. No. F6178), 1% penicillin/streptomycin (P/S, ThermoFisher Scientific, Waltham, MA, Cat. No. 15140122), and 0.1% gentamycin (Lonza, Walkersville, MD, Cat. No. 17-518Z). All cells were incubated at 37^0C in 5% CO_2 for propagation. Cell lines took time to grow, and this was dependent on the particular cell line. When the cells reached an appropriate number, the growth medium was aspirated off. We added 1 ml of trypsin (CORNING, Corning, NY, Cat. No. 25-053-C1) to the cells in a T-25 flask and incubated at 37^0C for three minutes. This helped the attached cells to come off the bottom of the flask. 1 ml of DMEM was added to the cells already incubated with trypsin. Next, the cells were centrifuged at 500 x g for five minutes. The

supernatant was aspirated off the cell pellet and discarded. The cell pellet was resuspended in a volume of DMEM, vortexed so that the cells mixed uniformly in the growth medium.

Growth rate and Confluence (%) of HT22 and HCN-2

HT22 mouse hippocampal cells (14th passage) and HCN-2 human cortical cells (6th passage) were grown in 96-well plate. The cells were treated with 20 μl trypsin (CORNING, Corning, NY, Cat. No. 25-053-C1), and were allowed to come off the bottom of the plate. It was then resuspended in 20 μl DMEM (CORNING, Corning, NY, Cat. No. 10-013-CV), mixed thoroughly by vortexing, and the total number was assessed using a hemacytometer (Hausser Scientific, VWR, Radnor, PA, Cat. No. 23649-061). From the total cell count, growth rate and % confluence was studied for both cell types. 100% confluence was estimated if the number of cells reached 40,000 in one of the wells of a 96-well plate. Initially, 2000 cells each of HT22 and HCN-2 were seeded in the 96-well plate. After every 24 hours for 9 days, the cells were counted for growth rate and confluence (%).

$$\textbf{Growth rate} = \sqrt[\textbf{n}]{\textbf{Total number of cells on nth day} \div \textbf{Total cells seeded initially}}$$

$$\textbf{where 'n' denotes the number of days.}$$

Cell viability assays

Neurobasal medium (Gibco, Invitrogen, Carlsbad, CA, Cat. No. 21103049) was added to WH1 and WH2 cell lines that were differentiated after 48 hours. In 100 ml Neurobasal medium, 1 ml N-2 Supplement (100X) and 2 mM L-glutamine was aseptically added. Next, the differentiated cells were seeded in a 48-well plate. Two repeats each of WH1 subclone (WH1 2 and WH1 3)

and WH2 subclone (WH2 1 and WH2 2) were considered for this assay. Doxycycline (1:1000 dilution in DMEM) was added eventually and the cells were kept in the CO_2 incubator for 72 hours. This step helped to induce the production of green fluorescent protein (GFP) in WH1 and WH2 cells and amyloid-beta protein (Aβ) in WH2 cells. Cell viability assay was performed using Annexin V-Cy3 Apoptosis kit (BioVision, Milpitas, CA, Cat. No. K102-25). The DMEM was aspirated off and the cells were resuspended in 250 μl of 1X Annexin Binding Buffer. 2.5 μl of Annexin V-Cy3 was added and incubated for 10 minutes in dark. Finally, the cells were observed under a fluorescent microscope using a rhodamine filter. The apoptotic cells gave faint red color, while the dead ones were bright red. On the other hand, the live cells did not fluoresce at all.

Next, cell lines WH8, WH9, and HT22 (control) were differentiated using neurobasal medium. The cells were eventually seeded (~ 125000) in a 6-well plate. 20 μM Aβ$_{1-42}$ was added from 1 mM Aβ$_{1-42}$ stock to the three wells containing WH8, WH9, and HT22. The other three wells of the plate had only DMEM without Aβ. The cells were kept in the CO_2 incubator for 48 hours. After the incubation period, cell viability was performed using 0.4% Trypan Blue Solution (Amresco, Solon, OH, Cat. No. K940). The cells were trypsinized and resuspended in 1 ml DMEM after which they were centrifuged at 500 x g for five minutes. The supernatant was aspirated off and the cell pellet was dissolved and mixed thoroughly in 180 μl of phosphate buffer saline (PBS, HyClone, Logan, UT, Cat. No. SH30256.01). Finally, 20 μl of 0.4% Trypan Blue Solution (1:10 volume of PBS) was added to the cells. The cells were incubated for 10 minutes after which they were counted using a hemacytometer. The dead cells were stained blue by the stain, while the live cells were clear and translucent.

Differentiated HT22 cells were seeded (~ 40000) in a 48-well plate. Following day, the cells were transfected chemically with AIRAP DsiRNA (Integrated DNA Technologies, IDT, Coralville, IA, Cat. No. N001159908.1, N133349.12.3, and N133349.12.1) and AIRAPL DsiRNA (IDT, Coralville, IA, Cat. No. N001159905.1, N026846.12.12, and N001159906.1) along with negative control (NC-1, IDT, Coralville, IA, Cat. No. 51-01-14-04). 2.1 µl each of AIRAP DsiRNA, AIRAPL DsiRNA, and NC-1 from 50 µM stocks were added to the cells. After 24 hours, the transfected cells were transferred from 48-well plate to 6-well plate. Finally, 20 µM Aβ$_{1-42}$ was added from 1 mM Aβ$_{1-42}$ stock to three wells containing HT22/AIRAP DsiRNA, HT22/AIRAPL DsiRNA, and HT22/NC-1. The other three wells containing the same set of cells did not have Aβ in them. The cells were incubated for 48 hours, after which they were stained using 0.4% Trypan Blue Solution and the cells were counted using a hemacytometer, following the same protocol that was used with cells lines WH8 and WH9.

RNA isolation

Doxycycline was added to WH1 (subclones 2 and 3), WH2 (subclones 1 and 2), HT22 cells and were seeded in a 6-well plate. WH1 and WH2 cells were harvested after 4, 8, 12, and 16-hour interval and HT22 cells were harvested after 0, 4, 8, 12, and 16-hour interval in 500 µl TRI Reagent Solution (RNA isolation reagent, Invitrogen, Thermo Fisher Scientific, Carlsbad, CA, Cat. No. AM9738). 50 µl of 1-Bromo-3-Chloropropane (Sigma-Aldrich, St. Louis, MO, Cat. No. B9673) was added to the samples in microcentrifuge tubes. The tubes were shaken vigorously for 30 seconds after which they were incubated for 3 minutes at room temperature. Next, the samples were centrifuged at 12000 x g for 15 minutes. The supernatant was transferred to another set of tubes that already had 250 µl of 2-Propanol (Sigma-Aldrich, St. Louis, MO, Cat.

No. I9516). The tubes were thoroughly vortexed after which the samples were incubated for 10

minutes at room temperature. Eventually, samples were centrifuged at 12000 x g for 10 minutes.

The supernatant was aspirated off and the pellet was washed with 500 µl of 75% ethanol.

Samples were again centrifuged at 7500 x g for 5 minutes. The pellet was let to dry and finally it

was dissolved in 50 µl of RNase free water. The samples were incubated at 55^0C water bath for

10 minutes before further analysis.

cDNA synthesis and Real-Time PCR

The RNA samples were next used to make copies of complementary DNA (cDNA) using the

manufacturer's instructions (Takara, Mountain View, CA, Cat. No. RR037A). The cDNA

samples were used to test the expression of AIRAP and AIRAPL using mouse AIRAP

(PrimeTime qPCR Primers, IDT, Coralville, IA, Cat. No. 127013791) and AIRAPL (qPCR-

AIRAPL-Ms-F, qPCR-AIRAPL-Ms-R, IDT, Coralville, IA, Cat. No. 114282272 and

114282273) primers, besides using the housekeeping primers, PGK1 (qPCR-PGK1-Ms-F,

qPCR-PGK1-Ms-R, IDT, Coralville, IA, Cat. No. 114282325 and 114282324) and RPS18

(qPCR-RPS18-Ms-F, qPCR-RPS18-Ms-R, IDT, Coralville, IA, Cat. No. 114282323 and

114282322). We used SYBR Select Master Mix dye (Applied Biosystems, Life Technologies,

Austin, TX, Cat. No. 4472897) to perform real-time PCR (StepOnePlus, Applied Biosystems,

Waltham, MA, Cat. No. 4376300) and study the expression levels of AIRAP and AIRAPL.

Statistical Analysis

Two-sample student t-test assuming unequal variances was performed to test if significant results were obtained in the experiments. Differences between experimental groups were considered statistically significant if the P-value was ≤ 0.05.

Characterization of HT22 and HCN-2 cells

To characterize HT22 (14th passage) and HCN-2 (6th passage) cells, the cell number, growth rate, and confluence (%) were recorded for nine days at 24-hour intervals. As shown in Figure 9A and 9B, starting with 2000 cells at day "0", both cell types continued to grow until the 9th day, although the rate of proliferation decreased at day "6" (HT22) and day "7" (HCN-2).

A

B

Figure 9. Characterization of HT22 and HCN-2 cells. Both HT22 **(A)** and HCN-2 **(B)** were seeded at 2,000 cells/well in 96-well plate. All cells were incubated overnight and counted after every 24 hou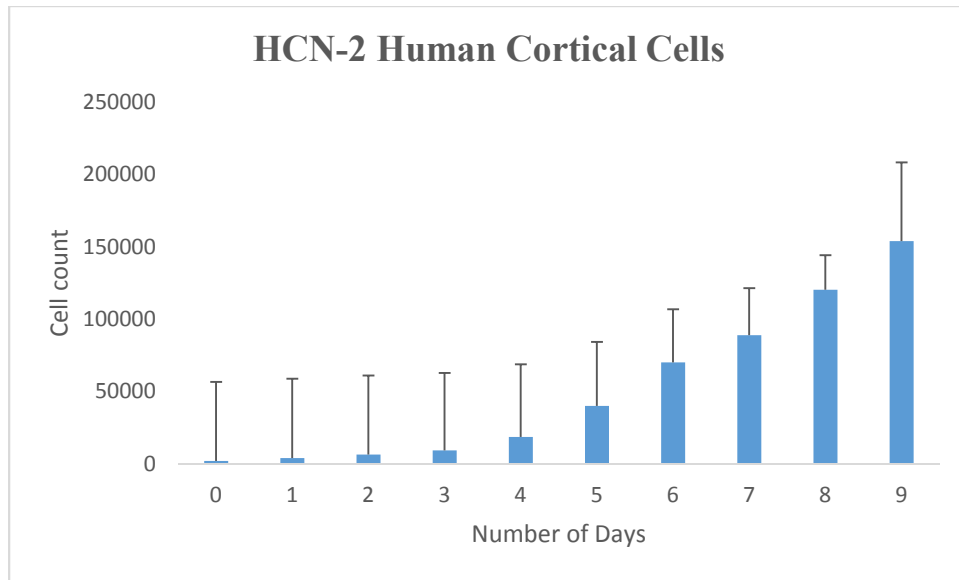rs, right after they were seeded. Cells were collected by trypsinization, and total cells were counted using a hemacytometer.

Next, as shown in Figure 10A and 10B, the growth rate of HT22 and HCN-2 cells were calculated from the total cell number for nine days. It was observed that the growth rate of HT22 was decreased after day "5". This could be primarily due to the increase in number of cells with time in the 96-well plate. This showed that the cells started dividing and after a certain point when they were many as compared to the area of the 96-well plate, they stopped dividing. The growth rate of HCN-2 was analyzed and found that after day "6", the cells started to divide slowly and hence their growth rate was lowered as compared to the days in the beginning.

A

B

Figure 10. Growth rate of HT22 and HCN-2 cells. Growth rate was calculated for nine days from the total cell count. For HT22 **(A)**, it was similar right from the beginning, but after day "5", it decreased till the last day. In case of HCN-2 **(B)**, the growth rate was reduced after day "6".

As shown in Figure 11A and 11B, the confluence (%) of HT22 and HCN-2 cells were calculated

from the total cell count. This was done in order to see the effect of confluence on cell growth.

It is estimated that if the total cell count was 40,000 in one of the wells of the 96-well plate, the

confluence would be 100%. Based on that, the confluence was calculated for both HT22 and

HCN-2 cells for nine days. On day "0", both HT22 and HCN-2 cells had 5% confluence as 2000

cells were seeded on that day. The confluence reached 65.81% on day "3" and went up to 135.5% on day "4", for HT22 cells, since the number of cells were 54,200. The confluence was found to be 397.5% on day "9", since the total number of cells were 159,000. Similarly, the confluence of HCN-2 was 100.08% on day "5", as number of cells were 40,033. On day "9", the confluence was found to be 385.12%, the number of cells being at 154,048. The confluence had a direct effect on the growth rate, for HT22, it went from 235.75% to 276.25% from day "5" to day "6". Also, for HCN-2, the confluence was 175.12% on day "6", and 222.50% on day "7". This showed that the confluence did not increase in the same way as on the initial days after seeding in both cell types. As a result, the growth rate was lowered after day "5" in HT22 and after day "6" in HCN-2 cells.

A

B

Figure 11. Confluence (%) of HT22 and HCN-2 cells. Confluence was calculated for nine days based on: 40,000 cells/well = 100% confluence. There was an increase in the confluence of both HT22 and HCN-2 cells, each day, through nine days. But, the increase in confluence was lowered after day "5" in HT22 **(A)**, and day "6" in HCN-2 **(B)**, that in turn affected the growth rate in both cell types.

Toxicity of Aβ on the neuronal cells

WH1 (control) and WH2 cell lines were used for cell viability assay using Annexin V-Cy3 Apoptosis kit. We used doxycycline-inducible system to trigger the production of Aβ. Doxycycline was added to both cell lines that were differentiated and incubated for 3 days. The apoptotic cells were stained red by the stain and cell viability (%) was calculated based on the number of dead cells present.

Table 1: % dead of differentiated WH1 and WH2 subclones with 72-hour Doxycycline treatment.

Name of subclones	Total Cells	Dead Cells	% Dead
WH1 2	308	1	0.32
WH1 3	432	2	0.46
WH2 1	229	6	2.62
WH2 2	282	7	2.48

The WH2 cells were sicker (most likely due to the presence of Aβ) than the WH1 cell lines, as evident under the microscope. Some of them died after the incubation period in presence of doxycycline, and so, we calculated the number of viable cells present. However, most of the WH2 cells did not die, but were sicker and had undergone apoptosis as compared to the WH1 subclones, which was evident from the calculated higher % dead after staining. The apoptotic and dead cells fluoresced red, while the live cells had no fluorescence.

AIRAP/AIRAPL protection against Aβ toxicity

Cell lines WH8, WH9, and HT22 (control) were used to study the protection of AIRAP/AIRAPL against Aβ. Aβ was added extracellularly and the differentiated cells were stained with Trypan Blue Solution after 2-day incubation.

Table 2: % dead cells in differentiated WH8, WH9, and HT22 after adding Aβ extracellularly and incubating for 2 days. Both WH8 and WH9 (6.40% and 6.57% respectively) had fewer dead cells compared to HT22 cells (8.04%).

Name of Cell Lines	Total Cells	Dead Cells	% Dead
WH8 (without Aβ)	236	12	5.08
WH8 + Aβ	125	8	6.40
WH9 (without Aβ)	507	16	3.15
WH9 + Aβ	350	23	6.57
HT22 (without Aβ)	1700	148	8.70
HT22 + Aβ	1193	96	8.04

The percentage of dead cells was calculated in the presence and absence of Aβ. % dead in WH8 and WH9 in presence of Aβ was found to be 6.40 and 6.57 respectively. Additionally, % dead in HT22 cells (control) in presence of Aβ was 8.04. This data is consistent with protection offered by AIRAP (WH8) and AIRAPL (WH9), since both cell lines had lower numbers of dead cells than the HT22 cells. However, the number of HT22 cells were way higher than both WH8 and WH9 during the time of counting. Moreover, HT22 cells without Aβ had higher % dead than HT22 with Aβ, which was most likely due to experimental variations.. This and the lack of repeats make this experiment hard to interpret.. Future experiments, should include multiple repeats of each condition- preferably 4 or more- and a standardized cell number and density. The inclusion of HT22 expressing an irrelevant protein (e.g. GFP or DsRed) as an additional control would also be advisable.

Effect of AIRAP/AIRAPL knockdown on Aβ toxicity

Differentiated HT22 cells were used to knockdown the expression of AIRAP and AIRAPL with

help of specific DsiRNA. Negative control (NC) was used where AIRAP and AIRAPL

expression was not targeted. . Aβ was added extracellularly and the cells were stained with

Trypan Blue Solution after a 2-day incubation.

Table 3: % dead cells when AIRAP and AIRAPL expression have been knocked down in presence of extracellular Aβ. The cells where AIRAP and AIRAPL expressions were knocked down had more dead cells (12.92% and 15.71% respectively) compared to the NC, where the expressions were restored.

Name of Cell Lines	Total Cells	Dead Cells	% Dead
HT22/AIRAPi (without Aβ)	1382	142	10.27
HT22/AIRAPi + Aβ	1416	183	12.92
HT22/AIRAPLi (without Aβ)	1460	108	7.39
HT22/AIRAPLi + Aβ	1012	159	15.71
HT22/NC (without Aβ)	2154	257	11.93
HT22/NC + Aβ	1510	145	9.60

The percentage of dead cells was calculated both in presence and absence of Aβ. Cells where

AIRAP and AIRAPL expression were knocked down and treated with Aβ (HT22/AIRAPi + Aβ

and HT22/AIRAPLi + Aβ), had 12.92% and 15.71% dead cells respectively, whereas HT22/NC

+ Aβ had 9.60% cells that were dead. This is consistent with our hypothesis that knockdown of

AIRAP/AIRAPL increases cell death, thus lowering the number of viable cells. However, there

were higher numbers of dead cells in HT22/NC in absence of Aβ (11.93%) than in presence of

Aβ (9.60%), although there were more number of cells in HT22/NC than in HT22/NC + Aβ,

which could account for higher dead cells at the end of incubation period. It is not possible to

interpret this data in the absence of experimental repeats. Therefore, additional experiments are needed before a final conclusion can be made.

Expression of AIRAP and AIRAPL in response to induced Aβ

Real-time PCR was performed on WH1 (subclones 2 and 3) and WH2 (subclones 1 and 2) that were treated with doxycycline and harvested after 4, 8, 12, 16, 24, and 48-hour interval (T4-T48). Both WH1 (denoted by "GFP") and WH2 (denoted by "Aβ") were treated in the absence of doxycycline and harvested right away after seeding (T0). It was observed that expression of AIRAP (Figure 12A) in WH2 cells was increased at 4 and 8-hour interval when compared to WH1 cells, although the increase was not statistically significant (P-value ≤ 0.7402). At 12-hour interval, the expression level was similar in both WH1 and WH2 cells with an increased AIRAP level in WH1 cells at the 16-hour interval. However, AIRAP expression was not enhanced in WH2 cells at 16-hour interval. By the end of 24 and 48-hour interval, it was observed that the expression dropped drastically in both WH1 and WH2 cells. Also, at T0, the expression was lowered in WH2 cells.

As shown in Figure 12B, there was a steady increase in the expression of AIRAPL in WH2 cells as compared to WH1 cells at 0, 4, 8, and 12-hour interval, although the change was not statistically significant (P-value ≤ 0.5048). However, AIRAPL expression was reduced in WH2 cells as compared to WH1 at 16, 24, and 48-hour interval.

A

B

Figure 12: Time-course experiment showing expression of AIRAP (A) and AIRAPL (B) in WH1 and WH2 cells at 0, 4, 8, 12, 16, 24, and 48-hour interval with doxycycline treatment. WH2 cells had enhanced AIRAP expression than WH1 at 4 and 8-hour interval while AIRAPL expression was enhanced at 0 till 12-hour interval in WH2. AIRAP expression was increased in WH1 cells at the 16-hour interval, while AIRAPL expression was enhanced in WH1 cells at 16, 24, and 48-hour interval. The data was normalized to WH1 T0 for both AIRAP and AIRAPL.

Furthermore, we wanted to study AIRAP and AIRAPL expressions in absence of Aβ induction in WH1 (GFP) and WH2 (Aβ) cells to confirm that any changes in AIRAP and AIRAPL expression levels found after induction were due to the expression of the transgene, rather than inherent differences between the two cell lines. It was shown that there were no statistically significant differences in AIRAP and AIRAPL expression between uninduced WH2 and WH1 cells. (Figures 13A and 13B).
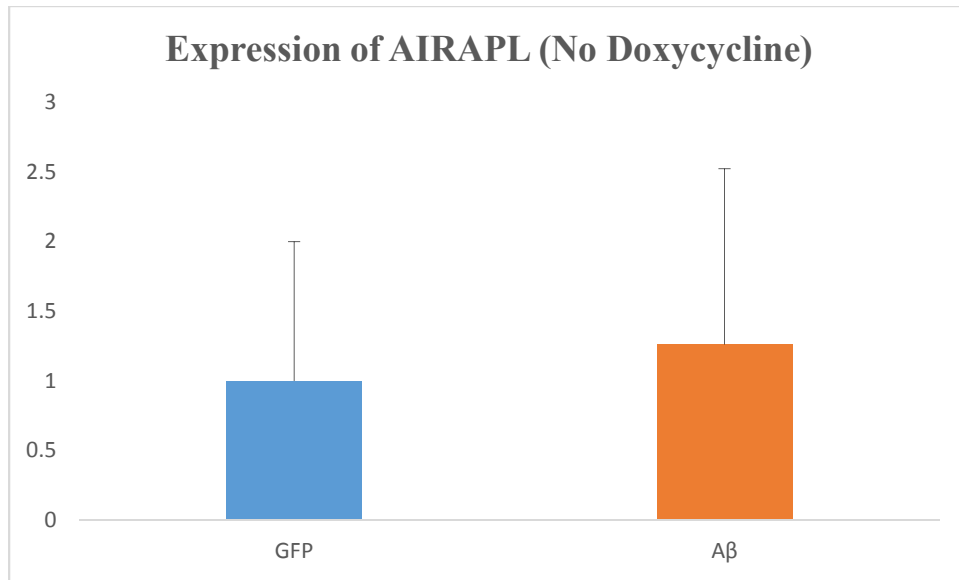
A

B

Figure 13: AIRAP (A) and AIRAPL (B) expressions in WH1 and WH2 cells in absence of doxycycline. WH2 cells had moderate increase in expression of AIRAP and AIRAPL than WH1 cells.

DISCUSSION

In this study, we hypothesized that AIRAP and AIRAPL could have a protective effect on the toxicity related to Aβ in mouse hippocampal cells. We used cell lines, WH1 and WH2, to determine the toxicity of Aβ. We may have found higher percentage of apoptotic and dead cells in WH2 than in WH1 after inducing the production of Aβ in WH2 cells via doxycycline. Although, doxycycline helped to induce Aβ intracellularly in WH2, the cells were not completely abolished after 3-days incubation period. However, most of the cells went into apoptotic stage, which was evident from the red fluorescence of the cells when stained with Annexin V. The WH2 cells appeared sicker than WH1. The live or the healthy cells were not stained at all, this was more frequently seen in WH1 cells, since the cell line did not have Aβ in them. We also used WH1 and WH2 cells without adding doxycycline in order to prevent the production of Aβ. It was found that the viability of WH1 and WH2 cells were similar after the incubation period. This was due to inability of WH2 cells to produce Aβ in absence of doxycycline, thus the cells were healthier and more viable.

Next, we wanted to study the effect of AIRAP and AIRAPL overexpression on Aβ toxicity. We used cell lines, WH8 and WH9, where AIRAP and AIRAPL were overexpressed using a CMV constitutive promoter. After treating the cells with $A\beta_{1-42}$, it was found that there were fewer dead cells in WH8 and WH9 compared to the HT22 cells that were treated with $A\beta_{1-42}$ as well. This conclusion is consistent with our hypothesis that AIRAP/AIRAPL overexpression could have a protective effect on the Aβ toxicity. One major drawback related to this particular conclusion could be the presence of fewer cells in WH8 and WH9 as compared to the HT22 cells after the incubation period. This might be due to the different rate of growing of HT22 and

36

WH8/WH9 cells. Furthermore, it was also found that the cells treated with $A\beta_{1-42}$ had lesser number of cells after the incubation period as compared to the cells without $A\beta_{1-42}$, although, equal number of cells were seeded at the beginning of the experiment. This could be due to $A\beta$ inhibiting the normal growth of cells. Moreover, it was found that there were higher number of dead cells in HT22 without $A\beta$ than in HT22 with $A\beta$ due to experimental variations, although, $A\beta$ is known to be toxic to the hippocampal cells. Besides, we did not use more repeats of WH8, WH9, and HT22 with/without $A\beta$, which would have helped to get a conclusive result.

Additionally, we wanted to study viability of cells after knocking down AIRAP/AIRAPL expression to confirm that AIRAP/AIRAPL were actually responsible for the protection against $A\beta$. We used HT22 cells and knocked down AIRAP and AIRAPL expression with help of specific DsiRNA. Eventually, the cells were treated with $A\beta_{1-42}$ and stained using Trypan Blue Solution. Higher percentage of the number of dead cells appeared to be in cells where the expression of AIRAP/AIRAPL was knocked out (HT22/AIRAPi + $A\beta$ and HT22/AIRAPLi + $A\beta$) as compared to cells having intact expression of both the genes. In other words, presence of AIRAP and AIRAPL contributed to higher number of viable cells that was shown in HT22/NC + $A\beta$. Hence, it was inferred that in absence of AIRAP and AIRAPL, the condition of the cells worsened and so we got more number of dead cells. However, we should have used more repeats of the cell lines in order to provide a more detailed explanation of the protection offered by AIRAP/AIRAPL against $A\beta$ toxicity. Future studies should aim to consider more repeats of each condition (AIRAP/AIRAPL knockdown, cell lines having intact expression of AIRAP/AIRAPL, as well as presence/absence of $A\beta$) to make a final conclusion.

Finally, we studied the gene expression of AIRAP and AIRAPL in presence of GFP and Aβ that was induced with help of doxycycline. WH1 and WH2 cells were treated with doxycycline at different intervals such as 4, 8, 12, 16, 24, and 48-hour. It was found that WH2 cells had higher levels of both AIRAP and AIRAPL (although not statistically significant) during the initial stages of induction of Aβ (4 and 8 hour) as compared to WH1. For the 12-hour treatment, both WH1 and WH2 cells had similar levels of AIRAP, although, AIRAPL expression was enhanced but not significantly in WH2 than in WH1 at 12-hour induction with doxycycline. But, it was found that by the 16-hour treatment with doxycycline, levels of AIRAP and AIRAPL decreased in WH2 than in WH1 cells. This could be due to the reduction of the effect of Aβ production with increase in the treatment time, thus lowering the gene expression levels. We also studied the expression levels in absence of doxycycline. It was shown that there were no statistically significant differences in AIRAP and AIRAPL expression levels in uninduced WH1 and WH2 cells. However, the time-course experiment at T0 showed lower AIRAP expression in WH2 than in WH1. Hence, more studies are required to get conclusive evidences about the expressions of AIRAP and AIRAPL in response to Aβ induction.

In the present study, we reported for the first time that AIRAP and AIRAPL could have protective effect against Aβ toxicity in mouse hippocampal cells. Through our findings and from other related studies, it is clear that Aβ is toxic to the mouse neuronal cells and the cells undergo apoptosis and eventually die in presence of Aβ. Cell lines that overexpress AIRAP/AIRAPL (WH8/WH9), appeared to offer protection against Aβ toxicity, thus helping in ameliorating the condition of the cells. Since, the experiment did not have more repeats, the findings could not be precise and definitive. Additionally, knockdown of both AIRAP/AIRAPL deteriorated the

condition of the cells, thus increasing the number of dead cells. Future studies should aim to consider more repeats of cell lines to get more conclusive results. Also, it would be interesting to study the effect of proteasome in the protection offered by AIRAP/AIRAPL against Aβ toxicity and thus could provide the potential mechanism for protection. Furthermore, we studied AIRAP/AIRAPL gene expression in cells having induced Aβ. It was noted that levels of AIRAP/AIRAPL were higher (not significant) at initial course of the experiment in cells having induced Aβ than in cells not having Aβ (having GFP alone). This finding suggested that AIRAP/AIRAPL was being produced in response to Aβ, which in turn helped to offer protection against the toxicity. However, with increase in the treatment time with doxycycline, the levels started to decline in response to Aβ. Finally, in future, it would be exciting to study the effect of AIRAP/AIRAPL in response to Aβ, added extracellularly to the HT22 cells.

References

1. Shackleton B., Crawford F., and Bachmeier C. "Inhibition of ADAM10 Promotes the Clearance of Aβ across the BBB by Reducing LRP1 Ectodomain Shedding." *Fluids and Barriers of the CNS*. BioMed Central, 2016.

2. Povova J., Ambroz P., Bar M, et al. "Epidemiological of and risk factors for Alzheimer's disease: A review." Biomed Pap Med Fac Univ Palacky Olomouc Czech Repub, 2012.

3. Cova I, Clerici F, Rossi A, et al. "Weight Loss Predicts Progression of Mild Cognitive Impairment to Alzheimer's Disease." *PLOS ONE* 11.3, 2016.

4. Scherling C S., Wilkins S E., Zakrezewski J, et al. "Decreased Self-Appraisal Accuracy on Cognitive Tests of Executive Functioning Is a Predictor of Decline in Mild Cognitive Impairment." Front Aging Neuroscience 8: 120, 2016.

5. Hasanbasic S, Jahic A, Karahmet E, et al. "THE ROLE OF CYSTEINE PROTEASE IN ALZHEIMER DISEASE." *Materia Socio-Medica*. AVICENA, D.o.o., Sarajevo, 2016.

6. Yin Y, Liu Y, Pan X, et al. "Interleukin-1β Promoter Polymorphism Enhances the Risk of Sleep Disturbance in Alzheimer's Disease." *PLOS ONE* 11.3, 2016.

7. http://www.medicalnewstoday.com/articles/159442.php

8. Hisham Q, and Kaddoumi A. "Effect of Mouse Strain as a Background for Alzheimer's Disease Models on the Clearance of Amyloid-β." *Journal of Systems and Integrative Neuroscience*. U.S. National Library of Medicine, 2016.

9. Cacace R, Sleegers K, and Van Broeckhoven C. "Molecular genetics of early-onset Alzheimer's disease revisited." *Alzheimer's & Dementia*. Elsevier, 2016.

10. Libro R, Diomede F, Scionti D. et al. "Cannabidiol Modulates the Expression of Alzheimer's Disease-Related Genes in Mesenchymal Stem Cells." *International Journal of Molecular Sciences* 18.1 (2016): 26.

11. Tapiola T, Alafuzoff I, Herukka S-K, et al. "Cerebrospinal Fluid β-Amyloid 42 and Tau Proteins as Biomarkers of Alzheimer-Type Pathologic Changes in the Brain." *Archives of Neurology* 66.3, 2009.

12. Tramutola A, Di Domenico F, Barone E, et al. "It Is All about (U)biquitin: Role of Altered Ubiquitin-Proteasome System and UCHL1 in Alzheimer Disease." *Oxidative Medicine and Cellular Longevity*. Hindawi Publishing Corporation, 2016.

13. Di Domenico F, Head E, Butterfield A. D., et al. "Oxidative stress and Proteostasis Network: Culprit and Casualty of Alzheimer's-Like Neurodegeneration." *Advances in Geriatrics*. Hindawi Publishing Corporation, 2014.

14. Pascale C. L., Miller M. C, Chiu C, et al. "Amyloid-beta Transporter Expression at the Blood-CSF Barrier Is Age-dependent." *Fluids and Barriers of the CNS*. Biomed Central, 2011.

15. Tseng B P., Green K. N., Chan J. L., et al. "Aβ Inhibits the Proteasome and Enhances Amyloid and Tau Accumulation." *Neurobiology of Aging*. U.S. National Library of Medicine, 2008.

16. Yun C., Stanhill A., Yang Y., et al. "Proteasomal adaptation to environmental stress links resistance to proteotoxicity with longevity in *Caenorhabditis elegans*." Proc Natl Acad Sci USA, 2008.

17. Hassan W. M., Merin D. A., Fonte V, et al. "AIP-1 ameliorates β-amyloid peptide toxicity in a *Caenorhabditis Elegans* Alzheimer's disease model." *Human Molecular Genetics*. Oxford University Press, 2009.

18. Ma C. J., Lee B, Weon J. B., et al. "Neuroprotective Compounds of Tilia Amurensis." *Pharmacognosy Magazine* 11.44, 2015.

19. Cho H. W., Jung S. Y., Lee G. H., et al. "Neuroprotective effect of *Citrus unshiu* immature peel and nobiletin inhibiting hydrogen peroxide-induced oxidative stress in HT22 murine hippocampal neuronal cells." *Pharmacognosy Magazine,* 2015.

20. Yun B. R., Yang H. J., Weon J. B., et al. "Neuroprotective Properties of Compounds Extracted from *Dianthus superbus* L. against Glutamate-induced Cell Death in HT22 Cells." *Pharmacognosy Magazine,* 2016.